JOURNAL OF AIRCRAFT
Vol. 36, No. 2, March–April 1999

Effects of Counterflow on the Aeroacoustic Properties of a Supersonic Jet

C. Shih,* F. S. Alvi,† and D. M. Washington‡
Florida A&M University and Florida State University, Tallahassee, Florida 32316-2175

The influence of counterflow on the mixing and acoustic characteristics of a Mach 1.4 rectangular jet operated at on- and off-design conditions were studied experimentally for different levels of counterflow. The results show that counterflow significantly enhances shear-layer mixing and reduces the jet potential core length under all operating conditions. Significant changes in both shock-cell spacing and strength were observed when counterflow was applied to nonideally expanded jets. Consequently, screech tones were either reduced or totally eliminated, and broadband shock-associated noise was shifted to higher frequencies. In the underexpanded mode, a Mach disk was formed at certain levels of counterflow, which substantially weakened the subsequent periodic shock-cell structure and reduced the broadband shock-associated noise and the overall sound pressure level (OASPL) by as much as 3 dB. Interestingly, it was also discovered that a jet operating at overexpanded conditions could be decelerated nearly isentropically by applying the proper amount of counterflow. This modification led to a 4 dB reduction in OASPL. Based on the present study, it is suggested that counterflow warrants further investigation as a potential noise reduction technique.

Introduction

IN recent years, researchers have investigated counterflow as a means to control the aerodynamic properties of jet flows.[1–6] In these studies, a secondary flow is applied to the periphery of a subsonic or supersonic jet to enhance mixing and/or to provide fluidic-based thrust vector control. It was shown by Strykowski et al.[1] that the mixing characteristics of an ideally expanded Mach 2 axisymmetric jet are significantly enhanced (by as much as 60%) when counterflow is applied to the jet periphery. Subsequent investigations utilized this technique to thrust vector a jet by selectively applying counterflow to isolated sections of the shear layer at the jet perimeter.[2–5] Van der Veer[2] was the first to use counterflow thrust vectoring (CFTV) to achieve pitch-vectoring of a subsonic rectangular jet. More recent studies showed that CFTV can be applied to supersonic jets to achieve single[3] and multiaxis[4,5] thrust vectoring. One of the advantages of this thrust-vectoring technique over its mechanical counterparts is that no moving parts are required. In addition, the secondary flow can provide thermal protection on the collar surface through film cooling. Hence, CFTV is less susceptible to the mechanical failure and heat transfer problems commonly experienced by currently available mechanical vectoring schemes.

The acoustic properties of a jet involving counterflow were first investigated experimentally by King et al.,[6] using a Mach 2 axisymmetric jet. This study revealed that the far-field overall sound pressure level (OASPL) decreased by 3 dB when counterflow was applied to the jet. Although these results are not extraordinary in terms of noise suppression, given the many potential benefits of counterflow, it is encouraging that application of counterflow does not impose noise penalty.

Presented as Paper 97-0149 at the AIAA 35th Aerospace Sciences Meeting, Reno, NV, Jan. 6–9, 1998; received Feb. 4, 1998; revision received Sept. 25, 1998; accepted for publication Oct. 1, 1998.

*Associate Professor, Department of Mechanical Engineering. Senior Member AIAA.

†Assistant Professor, Department of Mechanical Engineering. Member AIAA.

‡Graduate Research Assistant, Department of Mechanical Engineering. Student Member AIAA.

The focus of the earlier acoustic study[6] was to investigate jet noise at a constant nozzle pressure ratio [(NPR), defined as the ratio of the jet total pressure and the ambient pressure at the nozzle exit] at the nozzle design Mach number. However, in most practical applications, jets frequently operate at off-design conditions; hence, at different NPRs. When counterflow is applied to a jet periphery, it reduces the pressure at the nozzle exit. In the previous study,[6] the NPR was maintained constant at different levels of counterflow by reducing the jet stagnation pressure, thereby reducing its thrust.

In an effort to investigate the effect of counterflow on jet aeroacoustics under more realistic conditions, the present study was undertaken. In these experiments, a Mach 1.44 rectangular jet was used where the thrust was maintained nominally constant by keeping the jet stagnation pressure fixed. Furthermore, the effects of counterflow on a jet operating at overexpanded, underexpanded, as well as ideally expanded conditions, were also investigated, an area not explored in the earlier study.

It is generally accepted that supersonic jets have three components of noise.[7,8] These are 1) screech tones, 2) broadband shock-associated noise, and 3) turbulent mixing noise. Screech tones and broadband shock-associated noise are limited to supersonic jets operating at off-design conditions. This is because both of these components are produced as a result of the interaction of large-scale turbulent structures with the quasiperiodic shock-cell structure of a jet in the off-design condition. In one case, the acoustic waves from these interactions propagate upstream and further intensify the formation of the large-scale turbulent structures generated at the nozzle lip. The feedback loop caused by this process produces high-amplitude screech tones with discrete frequencies. Broadband shock-associated noise is simply the noise produced by the interactions of the shock cells and the large-scale turbulent structures. The large-scale turbulent mixing noise is produced by the shear-layer instabilities propagating at supersonic speeds relative to the ambient speed of sound. This is similar to the Mach wave radiation produced by a wavy wall traveling at supersonic speeds, as suggested by Tam.[8] The fine-scale turbulent mixing noise makes up the background noise in the jet. The excellent review article by Tam provides a more comprehensive discussion of the various components of supersonic jet noise.

The effects of counterflow on the various components of supersonic jet noise were studied by way of acoustic and aero-

dynamic measurements. In addition to the freejet (no counterflow) case, two levels of counterflow, moderate and strong, were also examined. Four stagnation pressures were investigated corresponding to the freejet fully expanded Mach numbers (M_j) of 1.3, 1.44, 1.6, and 1.8, corresponding to overexpanded, ideal, and two underexpanded cases. The Reynolds number ranges for these tests were 5×10^5 to 6.6×10^5, based on the small dimension of the rectangular jet.

Experimental Setup

The blowdown facility at the Fluid Mechanics Research Laboratory located at the Florida State University is used in the present study. This facility is capable of producing ideally expanded jets with Mach numbers in excess of 2.0, and stagnation temperatures up to 1000°F. The acoustic properties of the jet are measured in a 3.05 × 2.451 × 2.438 m anechoic chamber. This anechoic chamber has a cutoff frequency of 500 Hz. A two-dimensional traverse is used to position a 1/8-in. microphone in the far field of the jet.

A rectangular convergent–divergent nozzle with a design Mach number of 1.4 and an aspect ratio of 4 is used for the experiment. This nozzle converges and diverges in only one plane so that the width of the nozzle never changes. Based on the results of previous counterflow studies,[1–3] an optimized counterflow (or suction) collar was designed for the experiment. Figure 1 shows a schematic of the nozzle–collar geometry. To provide optical access for flow visualization, the side walls of the collar are made of acrylic plastic (Plexiglas®), whereas the upper and lower surfaces of the collar are equipped with glass windows. The small dimension (height, H) of the rectangular nozzle is 10.41 mm (0.41 in.) and the gap between the nozzle and the collar surface, at the nozzle exit, is ~50% of the nozzle height. The counterflowing current is produced by connecting the gaps in the suction collar by way of four hoses to a vacuum source. The vacuum source consists of two regenerative vacuum pumps, connected in series. With no suction, the pressure inside the collar was measured to be 14.2 psi, which was below the ambient room pressure of 14.6 psi.

Acoustic measurements obtained in this study were obtained, inside an anechoic chamber, along a circular arc at a radius of ~102 nozzle heights relative to the center of the collar exit plane. The acoustic measurements were made at 7.5-deg increments in a 90-deg arc. The measuring angle, χ, is defined as the angle measured clockwise from the jet centerline as indicated in Fig. 2, which shows a schematic of the arrangement inside the chamber. The measurements obtained along this arc between $\chi = 45-135$ deg were used to determine the effect of counterflow on the directivity and magnitude of various components of supersonic jet noise.

A personal computer, equipped with a data-acquisition card, was used to digitize and record the data. The acoustic data were collected by digitizing 320 K data points at a sampling rate of 250 kHz. A fast Fourier transform program was used to obtain the frequency spectrum with a bin size of 48 Hz. The flow was also qualitatively examined using flow-visualization methods. Integrated and instantaneous images of the flowfield were also obtained via conventional schlieren and shadowgraph techniques using a pulsed white light source. All of the flow visualization results were recorded using a high-resolution (1024 × 1024 pixels) digital charge-coupled device (CCD) camera.

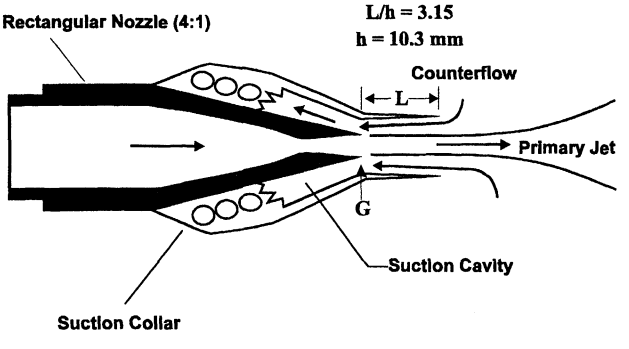

Fig. 1 Schematic of nozzle-collar assembly, side view.

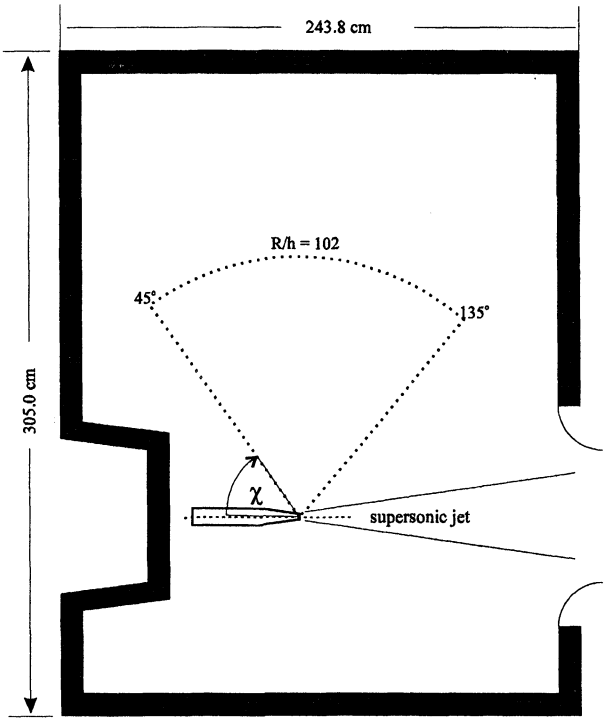

Fig. 2 Schematic of anechoic chamber.

Results and Discussion

Mixing Characteristics

The potential core length is one of the most frequently used indicators to quantify mixing characteristics of a jet. This length is defined as the distance measured from the nozzle exit to the location where the jet shear layers merge. This length can be determined with relative ease in ideally expanded jets, where the centerline Mach number remains constant until the shear layers merge, from which point the centerline Mach number decreases monotonically. Here, the end of the potential core was identified as the location where the centerline Mach number drops a certain level below the nozzle exit Mach number. This criterion for potential core length becomes harder to implement for jets operating at off-design conditions. For such cases, the presence of successive compression and expansion waves (shock cells) leads to significant fluctuations in the centerline Mach number distribution, making it difficult to clearly identify the end of the potential core. In an effort to overcome this difficulty, an average centerline Mach number was calculated by averaging locally the Mach number within each periodic shock cell. The potential core in this paper is then defined as the point where this locally averaged centerline Mach number begins to monotonically decrease below the averaged centerline Mach number measured near the nozzle exit. The averaged exit Mach number was calculated by averaging the Mach number distribution in the first four shock cells. In cases where a Mach disk was formed, the first four shock cells downstream of the Mach disk were used. Although this choice may appear to be somewhat arbitrary, other criteria for calculating the average Mach number, such as using a different number of shock cells, were also explored. They all yielded the same trend in terms of the potential core length. We recognize that, strictly speaking, potential flow precludes the presence of shock cells, by definition. However, the term potential

core is commonly used in literature to define the inviscid region upstream of the merging of the jet shear layers, and is so used in this paper.

The centerline Mach number distributions were obtained by measuring the pitot and static pressures along the centerline of the jet for different levels of counterflow at four stagnation pressures; the Rayleigh supersonic pitot formula was then used to calculate the centerline Mach number. In the collar region, reliable static pressure measurements could not be obtained because of probe interference effects. Consequently, Mach number distributions were measured at stations ~1.5 heights downstream from the nozzle exit. A representative case of the variation of the centerline Mach number for different levels of counterflow is shown in Fig. 3. The level of counterflow is represented by the absolute static pressure measured on the collar surface in the nozzle exit plane, denoted as P_G in the figure, where a lower P_G corresponds to higher counterflow. The jet is operating at a constant stagnation pressure of 84.5 psia, which is the most underexpanded condition investigated. The strong Mach number fluctuations are the result of the emergence of a periodic shock-cell structure that is typical of a jet operating at highly off-design conditions. The horizontal lines in the figure represent the average centerline Mach number for each level of counterflow, while the vertical lines signify the end of the potential core.

Figure 4 shows the variation of the potential core length as a function of stagnation pressure for various counterflow levels. In general, Fig. 4 shows that the application of counterflow decreases the potential core length for all operating conditions. Also, a reduction of potential core length occurs when the jet stagnation pressure decreases for all levels of counterflow. The reduction in potential core length caused by counterflow was

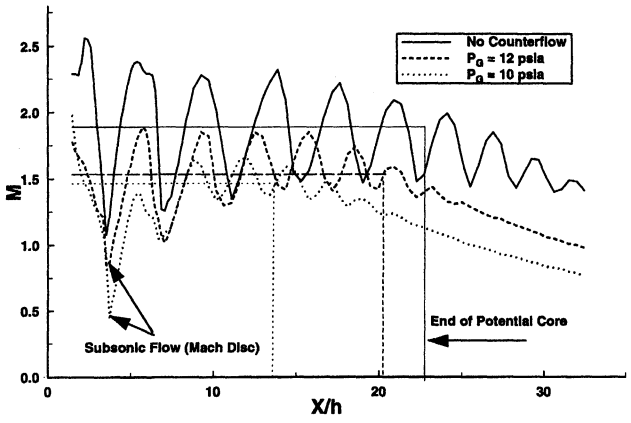

Fig. 3 Centerline Mach number distribution, P_0 = 84.5 psia.

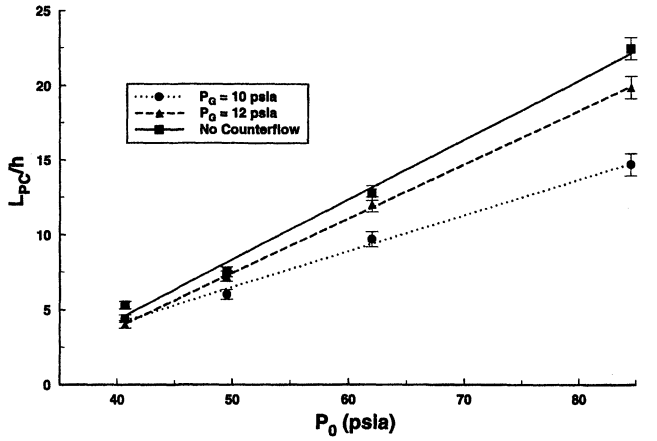

Fig. 4 Potential core length as a function of stagnation pressure and counterflow.

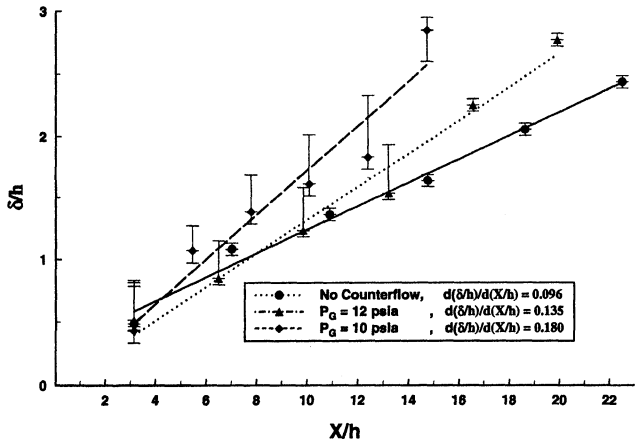

Fig. 5 Shear-layer growth for P_0 = 84.5 psia.

also observed by Strykowski et al.[1] for supersonic axisymmetric jets, and by Alvi et al.[9] for rectangular jets.

The shear-layer growth rate is another parameter that is normally used to quantify the shear-layer mixing level. The shear-layer growth rates were estimated via pitot pressure surveys across the jet shear-layer jet at several streamwise locations. The extent of the shear layer was determined by using the well-known 95–5% criteria. The shear layer inside the counterflow collar region consists of two parts: the fluid on the high-speed side flows in the forward direction, whereas that on the low-speed side flows in the opposite direction, thus creating a countercurrent shear layer. As a result, pitot surveys inside the counterflow collar would not provide an accurate measure of the shear-layer thickness, as they would only be sensitive to flow in the forward direction. To overcome this problem, growth rates were calculated from pitot surveys conducted downstream of the collar exit, where only the conventional forward-flowing shear layer is present.

Figure 5 shows a plot of the growth rate of an underexpanded jet with and without counterflow, where the shear-layer thickness is plotted vs streamwise location, nondimensionalized by the nozzle height, h. The three straight lines are obtained through a linear fit to each data set, where their slope indicates the trends observed in shear-layer growth. It is evident from the figure that higher levels of counterflow lead to significantly higher shear-layer growth rates. Such behavior was only observed for jets operating at underexpanded conditions. No conclusive data on the effect of counterflow on shear-layer growth could be obtained for overexpanded jets. This was because the potential core terminates a very short distance downstream of the counterflow collar exit, allowing for pitot surveys to be conducted at very few streamwise stations, thus making their interpretation difficult.

It should be noted that the application of counterflow results in minor thrust penalties caused by the vacuum pressures established in the collar region. The thrust loss is strongly dependent on the collar geometry, e.g., suction gap height, collar surface shape, etc. No direct measurements of thrust loss were made in the present study, but the interested reader can refer to Strykowski et al.[3] for a brief discussion of this aspect.

Flow Visualization

Flow visualization was used to gain a qualitative understanding of the shock-flow structure and the overall mixing characteristics of the jet. Instantaneous shadowgraph images of the jet at a stagnation pressure of 84.5 psia with and without counterflow are shown in Fig. 6, where the streamwise extent of each image is nominally 10 jet heights. White lines, approximately representing the divergence of the jet boundaries, are also included in the figure. Figure 6a shows the highly underexpanded jet without counterflow. A close examination of the image clearly reveals that a visible separation exists between

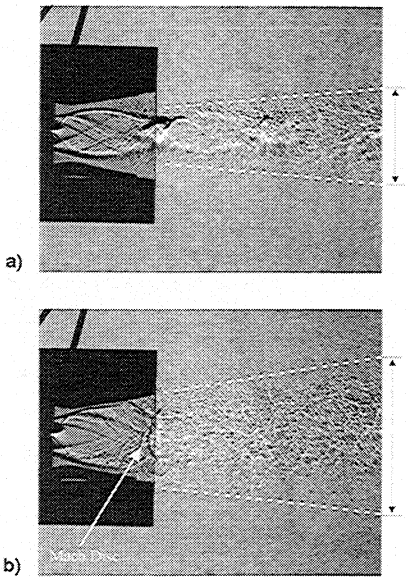

Fig. 6 Instantaneous shadowgraphs of an underexpanded jet, P_0 = 84.5 psia: a) no counterflow, M_j = 1.8, and b) with counterflow, P_G = 10 psia, M_j = 2.05.

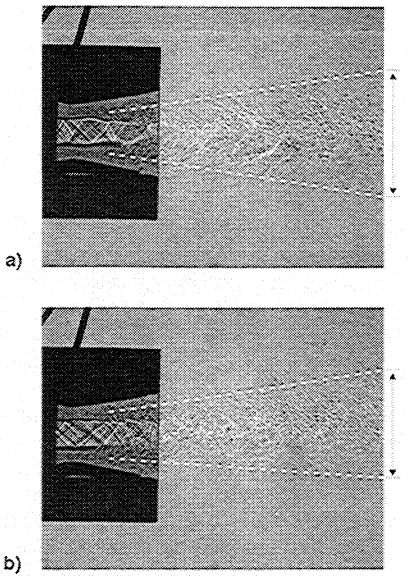

Fig. 7 Instantaneous shadowgraphs of an overexpanded jet, P_0 = 40.7 psia: a) no counterflow, M_j = 1.3, and b) with counterflow, P_G = 12 psia, M_j = 1.45.

the jet boundary and the collar surface inside the suction collar. However, when 10 psia of suction pressure is applied to the jet (Fig. 6b), the jet boundaries expand and appear to come into contact with the entire collar surface. This behavior is expected because the lower suction pressure inside the collar leads to a more underexpanded jet. For Fig. 6b, the fully expanded exit Mach number based on the ratio between the stagnation pressure and the suction pressure is estimated to be 2.05.

Upon comparing the two images shown in Fig. 6, it is clear that counterflow significantly increases the jet diffusion rate as indicated by the jet boundaries. This result is consistent with our earlier observations that the jet growth rate is increased and the potential core length is reduced as a result of counterflow. The significance of the enhanced mixing characteristics on the acoustic field of a jet will be discussed in more detail later.

Another noteworthy feature in Fig. 6b is the appearance of a vertically aligned structure inside the jet located close to the end of the collar (indicated by the arrow). Visually, this feature appears to be a Mach disk in the center of the jet. This observation is confirmed by the centerline Mach number survey of Fig. 3, which shows that the flow becomes subsonic at the same location; indicating the existence of a normal shock. The presence of a normal shock in the flow is significant because as Seiner and Norum[10] noted, the strength of shocks downstream of a normal shock are reduced significantly. Hence, the subsequent periodic shock cell structure is weakened. This observation is supported both by the shadowgraph images (Fig. 6) and the centerline Mach number distribution (Fig. 3). A more detailed discussion of the importance of the emergence of a Mach disk and its effect on the acoustic properties of a jet will be provided in a later section.

Corresponding shadowgraph images for an overexpanded jet with and without counterflow are presented in Fig. 7 for comparison. For the no-suction case (Fig. 7a), as the jet exits the nozzle, it goes through a contraction followed by an expansion inside the suction collar to adjust to the nonideal expansion condition. Farther downstream, strong periodic shock structures appear and the entire jet oscillates with the emergence of large-scale shear-layer structures. This behavior is well known for jets excited by screech tones. However, if a proper amount of counterflow is applied, the collar suction pressure can be adjusted to match the ideally expanded condition for the present configuration. Such an example is shown in Fig. 7b, where a 12-psia suction pressure is applied and the fully expanded Mach number for this pressure ratio is 1.45, which is very close to the design Mach number for the present nozzle. As expected, the jet column shows no noticeable contraction or expansion when exiting from the nozzle. The shock structures inside the jet are much weaker, with no apparent screech mode oscillation. This suggests that the counterflow technique can also be used to alter the ambient condition for an overexpanded jet, such that the jet can be operated at its design condition. This modification can lead to significant reduction of many undesired, shock-associated phenomena such as noise, structural vibrations, and thrust losses.

Shock-Cell Structure

The behavior of the periodic shock cell structure, normally quantified by the shock-cell strength and shock-cell spacing, is important because the interaction of the shock cells with the shear-layer turbulence has a primary influence on broadband shock-associated noise and screech tones. Centerline static pressure distributions are used to determine both the average shock-cell spacing and the average shock strength in the jet. Figure 8 shows an example of such a survey corresponding to the highly underexpanded case, where the presence of periodic compression and expansion waves is clearly visible by the series of pressure peaks and valleys. Each pressure rise represents the presence of a compression region, which is followed by an expansion zone, where the pressure decreases. The periodic shock pattern persists to more than 35 jet heights downstream for the case with no counterflow. The application of counterflow significantly reduces both the shock-cell strength and their spacing. Furthermore, the streamwise extent of the periodic shock-cell wave train is also significantly reduced.

The average shock-cell spacing is defined as the averaged distance between two adjacent valleys in the static surveys (alternatively, one may also use the distance between adjacent peaks). All of the shocks used in the calculation of the average spacing must have a minimum of 10% of the first shock's strength. This criterion is chosen to ensure a consistent result. Strictly speaking, shock-cell spacing is defined as the distance between adjacent points, where the shock/compression wave intersects the sonic line in the shear layer. However, for our purpose, where the goal is to compare the relative effect of counterflow on shock cell spacing, any consistent definition yields the same trend.

Figure 9 shows the average shock-cell spacing as a function of jet stagnation pressure for different counterflow levels. The

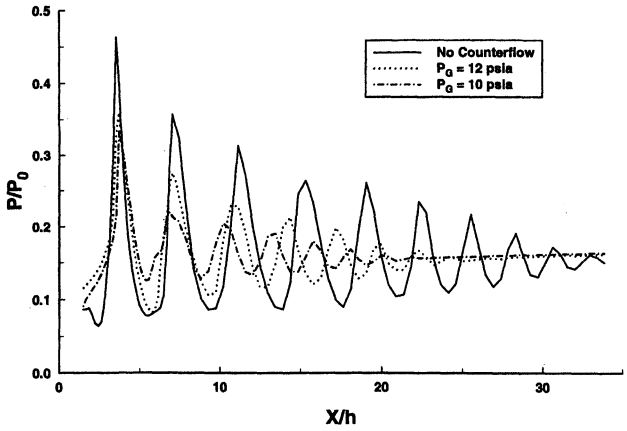

Fig. 8 Centerline static pressure distribution, P_0 = 84.5 psia.

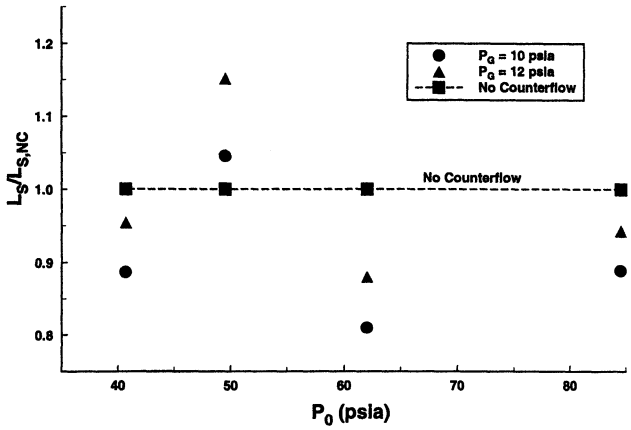

Fig. 9 Shock-cell spacing as a function of stagnation pressure and counterflow.

ordinate represents the shock-cell spacing L_S, normalized by the shock-cell spacing for the no-counterflow case, $L_{S,NC}$, at each stagnation pressure. It can be clearly seen that the average shock-cell spacing decreases when the level of counterflow increases for all stagnation pressures, except for the P_0 = 49.5-psia case. For this pressure, the jet without counterflow is operating close to the ideally expanded condition. Therefore, the use of suction decreases the collar pressure and causes the jet to become underexpanded, which drastically increases the shock cell spacing. However, from this point onward, any further increase in counterflow leads to a decrease in the spacing, consistent with the behavior observed at all other stagnation pressures.

The change of shock-cell spacing may be explained by the enhanced mixing in the jet shear layer caused by counterflow. It is speculated that the elevated mixing level causes the jet shear layers and the sonic line to converge toward the center of the jet. Therefore, the oblique expansion and compression waves traverse a shorter distance before they reflect off the shear layer, resulting in a decrease in the shock-cell spacing.

The average shock-cell strength in the jet affects both the broadband shock-associated noise and screech tones. The strength of shocks in the jet plume is related to the pressure mismatch between the exit pressure of the jet and the ambient pressure. Shocks form in the jet so that the static pressure of the jet can be adjusted to the ambient condition. Following the definition used by Seiner and Norum,[10] the shock-cell strength (denoted as ΔP_S in Fig. 10, to be discussed later), is defined as the difference between the centerline static pressure at the end of the compression region, i.e., a pressure peak, and the static pressure minimum at the beginning of the adjacent compression. Average shock strength is determined by averaging

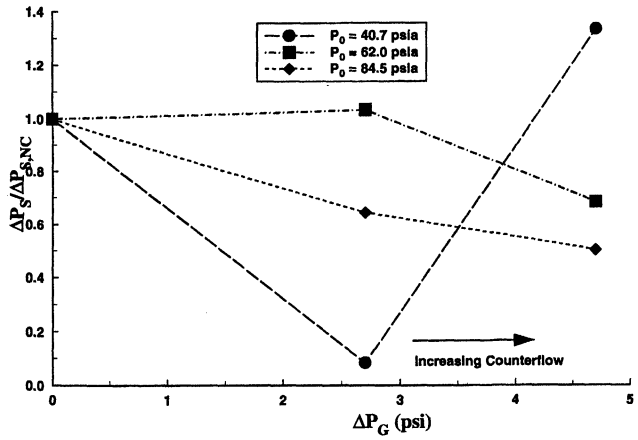

Fig. 10 Shock-cell strength as a function of stagnation pressure and counterflow.

the strength of all shocks that have a minimum of 10% of the first shock's strength.

A plot of the average shock-cell strength vs the counterflow level is shown in Fig. 10. The parameter, ΔP_G is the difference between the ambient atmospheric pressure and the gap pressure P_G (defined earlier); hence, increasing ΔP_G represents increasing counterflow. At each stagnation pressure, the shock-cell strength ΔP_S has been normalized by the shock-cell strength with no counterflow $\Delta P_{S,NC}$. Although they carry no physical significance, dotted lines were included for visual aid purposes. The behavior seen in this plot warrants some discussion. Starting with the overexpanded case (P_0 = 40.7 psia), one observes that as moderate counterflow is applied, the shock-cell strength decreases. This is because the application of moderate suction causes the jet to operate closer to the ideally expanded condition as compared with the no-counterflow condition. However, a further increase in the counterflow causes the jet to become underexpanded because of the pressure mismatch at the jet exit, which, in turn, leads to an increase in shock-cell strength. For the two remaining cases (P_0 = 62.0 and 84.5), the jet is always underexpanded and the shock-cell strength decreases with increasing counterflow.

In the case of the ideally expanded jet, corresponding to P_0 = 49.5 psia, the application of moderate suction causes the jet to become underexpanded, resulting in a dramatic increase in the shock-cell strength. A further increase in counterflow (or suction) leads to a drop in the normalized shock-cell strength. The initial increase in the shock-cell strength of the ideally expanded jet is almost four times the change in shock strengths observed for the three cases shown in this figure. As a result, data for this case are not included in Fig. 10, primarily because it would visually undermine the trends observed for the other three cases. In summary, the plot indicates that for an underexpanded jet, increasing counterflow will result in weaker shock cells. At first glance, this behavior may appear counterintuitive. One would expect that as P_G is reduced, i.e., counterflow is increased, the jets see a more drastic pressure mismatch at the exit, which should result in stronger shock cells. At this point, the reason for this behavior is not entirely clear, although one may speculate that by increasing counterflow we are enhancing the mixing rates in the jet shear layers, which somehow affects the local pressure distribution in the jet exit plane.

Acoustic Measurements

Figure 11 shows the power spectra of sound pressure level (SPL) of a highly underexpanded jet for several levels of counterflow. The measurements were taken at an angle of χ = 45 deg, where the presence of screech tones and broadband shock-associated noises were more prominent. When counterflow is not applied, a discrete peak, representing the screech

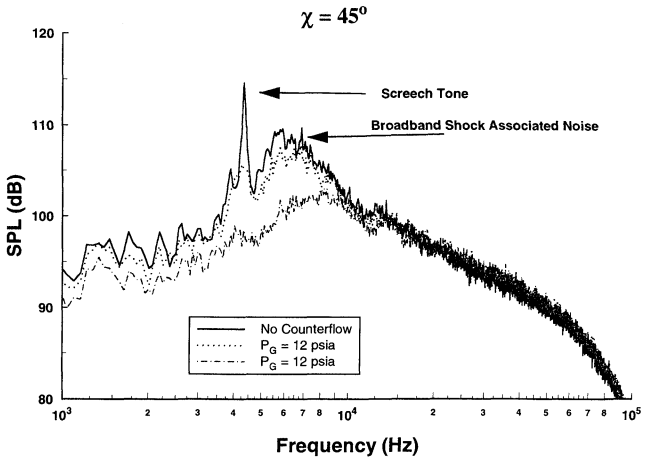

Fig. 11 SPL spectra for P_0 = 84.5 psia at χ = 45 deg.

mode, is present at a frequency of ~4100 Hz. For a moderate level of counterflow (P_G = 12 psia), the amplitude of the screech tone drops significantly, but its frequency remains unchanged. If the level of counterflow is further increased, it can be clearly seen that the screech tone is eliminated completely. This trend is not limited to this specific test condition; rather, screech tones are either reduced or eliminated by the use of counterflow for all test cases.

Although at present it is not entirely clear why counterflow suppresses screech tones in jets, there are several possible reasons worth considering. First, it is well accepted that screech tones are initiated near the nozzle exit, where the shear layer is very thin and inherent instability waves are receptive to external excitation.[8] However, in the presence of counterflow, the resulting elevated mixing levels in the jet shear layer cause the shear layer to become thicker everywhere, including the nozzle exit.[9] Consequently, the shear-layer instabilities would be less receptive to external forcing. Second, it is also known that the acoustic radiation that provides external forcing of the shear-layer instability at the nozzle exit is produced by the interaction of the amplified instability wave and the periodic shock cells. Because measurements presented earlier show that the strength of the shock cells is reduced dramatically with the application of counterflow (Figs. 8 and 10), it is reasonable to expect that the amplitude of the acoustic forcing would also be reduced. The net effect of either or both these mechanisms would be to weaken the feedback loop responsible for screech tones.

Recall that the broadband shock-associated noise is generated as a result of the interaction of the periodic shock-cell structure with the large-scale turbulent structures in the shear layer. This noise component can be identified as the broadened peak to the right of the screech tone in Fig. 11. When counterflow is increased, this component of supersonic jet noise shifts to a higher frequency and its magnitude decreases. The reason behind the frequency shift becomes clear if one recalls that increasing counterflow leads to reduced shock-cell spacing (Fig. 9). Consequently, shear-layer structures would interact with the shock cells more frequently, generating noise at higher frequencies. The fact that this component of jet noise moves to a higher frequency is encouraging because noise-suppression devices, such as the use of liners, are able to efficiently minimize high-frequency noise sources.

The decrease in the magnitude of broadband shock-associated noise may be explained as follows. As counterflow is applied to the jet the scale of the large-scale turbulent structures increases,[1,9] whereas the average strength of the shock cells decreases. In particular, for high levels of counterflow, a Mach disk appears in the jet column (Fig. 6b), significantly reducing the strength of the downstream shock cells. The reduced shock-cell strength in the jet causes the magnitude of the broadband shock-associated noise to decrease.

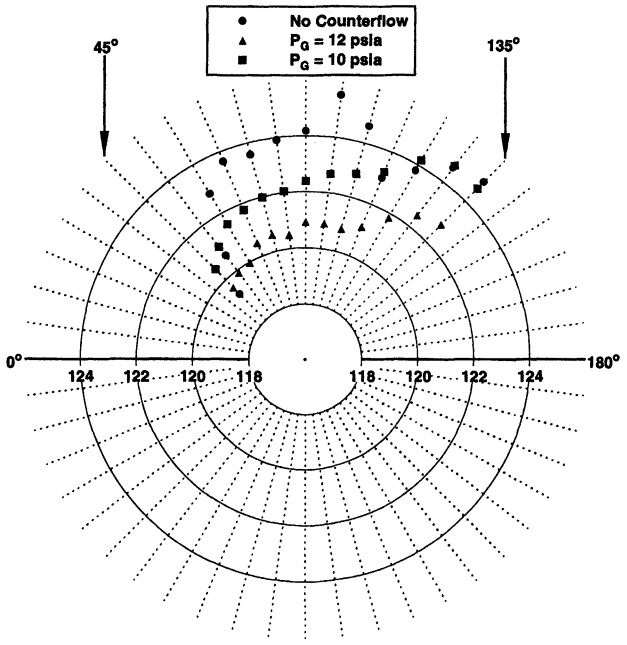

Fig. 12 Polar plot of OASPL for P_0 = 84.5 psia (underexpanded case).

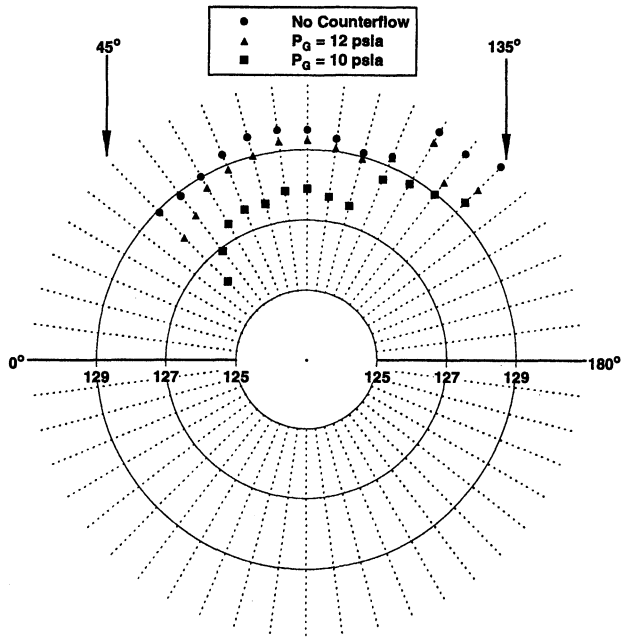

Fig. 13 Polar plot of OASPL for P_0 = 40.7 psia (overexpanded case).

The influence of counterflow on turbulent mixing noise can be surmised by examining the power spectra shown in Fig. 11. It appears that the large-scale mixing noise (corresponding to lower frequencies) decreases marginally, whereas the small-scale turbulent mixing noise (at high frequencies) is relatively unaffected. Although the overall turbulent mixing noise is not reduced, it is encouraging that counterflow does not significantly increase this component of jet noise.

So far we have examined the effect of counterflow on the various components of supersonic jet noise. In this section, we will discuss its net effect on the far-field noise as indicated by OASPL measurements. A polar plot of OASPL vs χ is shown in Fig. 12, where the jet is operating at a stagnation pressure of 84.5 psia for different levels of counterflow. For this case, it is evident that for moderate counterflow (P_G = 12 psia), there is a slight reduction in OASPL. For higher counterflow (P_G = 10 psia), the OASPL drops by almost 3 dB. More significantly,

this reduction is uniform at all angular locations. It is believed that this reduction is primarily a result of the decrease in broadband shock-associated noise presented earlier in Fig. 11.

The OASPL distribution for an overexpanded case is shown in Fig. 13. An initial decrease in the noise for low suction is observed (counterflow), followed by an increase for higher counterflow levels. This behavior of the OASPL follows the pattern exhibited by the shock-cell strength for this stagnation pressure, shown in Fig. 10. As discussed earlier, the shock cells become weaker as a low level of counterflow (P_G = 12 psia) is applied, because the jet operates closer to the ideal mode. Additional suction (P_G = 10 psia) causes the jet to become underexpanded, thereby increasing the shock-cell strength and the shock-associated noise, leading to a higher OASPL.

Conclusions

The effects of counterflow on the aerodynamic and acoustic characteristics of a Mach 1.4 rectangular jet were investigated. To examine the effects on turbulent mixing noise as well as shock-associated noise, the jet was operated at on- and off-design conditions at different levels of counterflow. The results show that counterflow significantly enhances shear-layer mixing and reduces the jet potential core length under all operating conditions.

Changes in both shock-cell spacing and strength occur when counterflow is applied to nonideally expanded jets. Screech tones are either reduced (for low levels of counterflow) or totally eliminated (for higher counterflow) and broadband shock-associated noise is observed to shift to higher frequencies. In the underexpanded mode, a Mach disk is formed at higher levels of counterflow, significantly weakening the subsequent periodic shock-cell structure. This reduces the broadband shock-associated noise and the OASPL by as much as 3 dB. It was also discovered that a jet operating at overexpanded conditions can be decelerated nearly isentropically by applying the proper amount of counterflow. This modification reduces the strength of the periodic shock cells, resulting in a 4-dB reduction in OASPL. Although the noise reduction is relatively modest, given the many potential benefits of counterflow, it is encouraging that the application of counterflow does not impose a noise penalty. Furthermore, the shift of broadband shock-associated noise to higher frequencies makes the use of noise-suppression devices such as acoustic liners potentially viable. Such noise-suppression schemes that employ counterflow need to be further explored.

Acknowledgments

The authors thank A. Krothapalli for his many insightful comments, and Edward Barber for his assistance in performing this experiment. The Grant provided by NASA Langley Research Center and NASA Headquarters for conducting this research is greatly appreciated.

References

[1]Strykowski, P. J., Krothapalli, A., and Jendoubi, S., "The Effect of Counterflow on the Development of Compressible Shear Layers," *Journal of Fluid Mechanics*, Vol. 308, Feb. 1996, pp. 63–96.

[2]Van der Veer, M. R., "Counterflow Thrust Vectoring of a Subsonic Rectangular Jet," M.S. Thesis, Dept. of Mechanical Engineering, Univ. of Minnesota, Minneapolis, MN, 1995.

[3]Strykowski, P. J., Krothapalli, A., and Forliti, D. J., "Counterflow Thrust Vectoring of Supersonic Jets," *AIAA Journal*, Vol. 34, No. 11, 1996, pp. 2306–2314.

[4]Alvi, F. S., Strykowski, P. J., Washington, D. M., and Krothapalli, A., "Multi-Axis Fluidic Thrust Vectoring of Supersonic Jets via Counterflow," AIAA Paper 97-0393, Jan. 1997.

[5]Washington, D. M., Alvi, F. S., Strykowski, P. J., and Krothapalli, A., "Multiaxis Fluidic Thrust Vector Control of a Supersonic Jet Using Counterflow," *AIAA Journal*, Vol. 34, No. 8, 1996, pp. 1734–1736.

[6]King, C. J., Krothapalli, A., and Strykowski, P. J., "The Effect of Annular Counterflow on Supersonic Jet Noise," CEAS/AIAA Paper 95-169, June 1995.

[7]Powell, A., "On the Mechanism of Choked Jet Noise," *Proceedings of the Physical Society of London*, Vol. 66, 1953, pp. 1039–1056.

[8]Tam, C. K. W., "Supersonic Jet Noise," *Annual Review of Fluid Mechanics.*, Vol. 27, 1995, pp. 17–43.

[9]Alvi, F. S, Washington, D. M., and Krothapalli, A., "Experimental Study of a Compressible Countercurrent Turbulent Shear Layer," *AIAA Journal*, Vol. 34, No. 4, 1996, pp. 728–735.

[10]Seiner, J. M., and Norum, T. D., "Aerodynamic Aspects of Shock Containing Jet Plumes," AIAA Paper 80-0965, June 1980.